Supporting information for:

Multifunctional RNA nanoparticles

Kirill A. Afonin[1], Mathias Viard[1,2], Alexey Y. Koyfman[3], Angelica N. Martins[4], Wojciech K. Kasprzak[2], Martin Panigaj[5], Ravi Desai[1], Arti Santhanam[1], Wade W. Grabow[6], Luc Jaeger[7], Eliahu Heldman[2], Jakob Reiser[5], Wah Chiu[3], Eric O. Freed[4], Bruce A. Shapiro[1#]

[1] Basic Research Laboratory, Center for Cancer Research, National Cancer Institute, Frederick, MD 21702, USA

[2] Basic Science Program, Leidos Biomedical Research, Inc., NCI Center for Cancer Research, Frederick National Laboratory for Cancer Research, Frederick, MD 21702, USA

[3] National Center for Macromolecular Imaging, Verna and Marrs McLean Department of Biochemistry and Molecular Biology, Baylor College of Medicine, Houston, TX 77030, USA

[4] HIV Drug Resistance Program, National Cancer Institute, Frederick, MD 21702, USA

[5] Food and Drug Administration, Center for Biologics Evaluation and Research, Office of Cellular, Tissue and Gene Therapies, Silver Spring, MD 20993, USA

[6] Department of Chemistry, Seattle Pacific University, Seattle, WA 98119, USA

[7] Department of Chemistry and Biochemistry, Biomolecular Science and Engineering Program, University of California, Santa Barbara, CA 93106-9510, USA

- to whom correspondence should be addressed: Bruce A. Shapiro, phone 301-846-5536; fax 301-846-5598; email: shapirbr@mail.nih.gov

Sequences used in this project

Bold letter sequences indicate kissing loop regions.

RNA nanorings 3′-side functionalized with Dicer substrate (DS) antisenses against enhanced Green Fluorescent Protein (eGFP S1[1, 2])

(((((((.......)))))))(((((((.......)))))))..........................
DS A_GFP
5′-GGGAACC**GUCCACU**GGUUCCCGCUACGAG**AGCCUGC**CUCGUAGCuucgguggugcagaugaacuucaggguca
DS B_GFP
5′-GGGAACC**GCAGGCU**GGUUCCCGCUACGAG**AGAACGC**CUCGUAGCuucgguggugcagaugaacuucaggguca
DS C_GFP
5′-GGGAACC**GCGUUCU**GGUUCCCGCUACGAG**ACGUCUC**CUCGUAGCuucgguggugcagaugaacuucaggguca
DS D_GFP
5′-GGGAACC**GAGACGU**GGUUCCCGCUACGAG**UCGUGGU**CUCGUAGCuucgguggugcagaugaacuucaggguca
DS E_GFP
5′-GGGAACC**ACCACGA**GGUUCCCGCUACGAG**AACCAUC**CUCGUAGCuucgguggugcagaugaacuucaggguca
DS F_GFP
5′-GGGAACC**GAUGGUU**GGUUCCCGCUACGAG**AGUGGAC**CUCGUAGCuucgguggugcagaugaacuucaggguca
Dicer substrate sense
5′-ACCCUGAAGUUCAUCUGCACCACCG

RNA nanorings 3′-side functionalized with Malachite Green (MG) aptamers[3, 4]

(((((((.......)))))))(((((((.......)))))))..((((((.........(((((....)))))...)))))))
A_MG
5′-GGGAACC**GUCCACU**GGUUCCCGCUACGAG**AGCCUGC**CUCGUAGCUUGACAUGGUAACGAAUGACAGUUCGCUGUCCGACAUGUC
B_MG
5′-GGGAACC**GCAGGCU**GGUUCCCGCUACGAG**AGAACGC**CUCGUAGCUUGACAUGGUAACGAAUGACAGUUCGCUGUCCGACAUGUC
C_MG
5′-GGGAACC**GCGUUCU**GGUUCCCGCUACGAG**ACGUCUC**CUCGUAGCUUGACAUGGUAACGAAUGACAGUUCGCUGUCCGACAUGUC
D_MG
5′-GGGAACC**GAGACGU**GGUUCCCGCUACGAG**UCGUGGU**CUCGUAGCUUGACAUGGUAACGAAUGACAGUUCGCUGUCCGACAUGUC
E_MG
5′-GGGAACC**ACCACGA**GGUUCCCGCUACGAG**AACCAUC**CUCGUAGCUUGACAUGGUAACGAAUGACAGUUCGCUGUCCGACAUGUC
F_MG
5′-GGGAACC**GAUGGUU**GGUUCCCGCUACGAG**AGUGGAC**CUCGUAGCUUGACAUGGUAACGAAUGACAGUUCGCUGUCCGACAUGUC

RNA rings 3′-side modified with six identical ssRNA toeholds

Toeholds are underlined.

(((((((.......)))))))(((((((.......)))))))............
A_toehold
5′-GGGAAUCC**GUCCACU**GGAUUCCCGUCACAG**AGCCUGC**CUGUGACuucgguggugca
B_toehold
5′-GGGAAUCC**GCAGGCU**GGAUUCCCGUCACAG**AGAACGC**CUGUGACuucgguggugca
C_toehold
5′-GGGAAUCC**GCGUUCU**GGAUUCCCGUCACAG**ACGUCUC**CUGUGACuucgguggugca
D_toehold
5′-GGGAAUCC**GAGACGU**GGAUUCCCGUCACAG**UCGUGGU**CUGUGACuucgguggugca
E_toehold
5′-GGGAAUCC**ACCACGA**GGAUUCCCGUCACAG**AACCAUC**CUGUGACuucgguggugca
F_toehold
5′-GGGAAUCC**GAUGGUU**GGAUUCCCGUCACAG**AGUGGAC**CUGUGACuucgguggugca
DS sense with toehold
5′-ACCCUGAAGUUCAUCUGCACCACCGUGCACCACCG
DS antisense
5′-CGGUGGUGCAGAUGAACUUCAGGGUCA

RNA nanoring 3′-side functionalized with DS antisenses against six different HIV-1[5]

The names of corresponding dicer substrates (DS) RNAs are indicated for each concatenated ring strand. Nanorings constructs contain a combination of six different DS RNAs that target the HIV-1 genome. Nanoring construct A targets: PBS-Matrix (PBS-MA), Envelope (gp120), Capsid (CA), Reverse Transcriptase (RT), Protease (PR) and Nef. Nanoring construct B targets: PBS-Matrix (PBS-MA), Capsid (CA), Reverse Transcriptase (RT), Protease (PR), Nef and Rev-Tat. Abbreviations: PBS, Primer Binding Site region; gp120, surface glycoprotein of 120KDa; Rev, Regulator of Expression Virion Proteins; Tat, Trans-Activator of Transcription; Nef, Negative Factor.

(((((((.......)))))))(((((((.......)))))))..........

For nanoring A

DS A_PBS-Matrix

5′-GGGAAUCC**GUCCACU**GGAUUCCCGUCACAG**AGCCUGC**CUGUGACuugacggacucgcacccaucucucuccuu

DS B_Envelope/gp120

5′-GGGAAUCC**GCAGGCU**GGAUUCCCGUCACAG**AGAACGC**CUGUGACuuggacaauuggagaagugaauuauauu

DS C_Capsid

5′-GGGAAUCC**GCGUUCU**GGAUUCCCGUCACAG**ACGUCUC**CUGUGACuuccuggaaugcugucaucauuucuucuu

DS D_Reverse Transcriptase

5′-GGGAAUCC**GAGACGU**GGAUUCCCGUCACAG**UCGUGGU**CUGUGACuuauuuaucuacuuguucauuuccucca

DS E_Protease

5′-GGGAAUCC**ACCACGA**GGAUUCCCGUCACAG**AACCAUC**CUGUGACuuucuucuaauacuguaucaucugcuccu

DS F_Nef

5′-GGGAAUCC**GAUGGUU**GGAUUCCCGUCACAG**AGUGGAC**CUGUGACuuggaggaaauuagcccuuccagucccuu

For nanoring B

DS B_Rev-Tat

5′-GGGAAUCC**GCAGGCU**GGAUUCCCGUCACAG**AGAACGC**CUGUGACuucgcugacuccgcuucuuccugccauuu

Corresponding DS senses(HIV-1)[5]

For nanoring A

DS PBS-Matrix

5′-pGGAGAGAGAUGGGUGCGAGUUCGUC

DS Envelope/gp120

5′-pUAUAAUUCACUUCUCCAAUUGUCC

DS Capsid

5′-pGAAGAAAUGAUGACAGCAUUUCAGG

DS Reverse Transcriptase

5′-pGAGGAAAUGAACAAGUAGAUAAAU

DS Protease

5′-pGAGCAGAUGAUACAGUAUUAGAAGA

DS Nef

5′-pGGGACUGGAAGGGCUAAUUUUCUCC

For nanoring B

DS Rev-Tat

5′-pAUGGCAGGAAGAAGCGGAGUUAGUG

RNA nanorings 3′-side functionalized with DS antisenses against GSTP1-1

(These constructs were used as negative controls in HIV-1 experiments)

DS A_GSTP1-1

5′-GGGAAUCC**GUCCACU**GGAUUCCCGUCACAG**AGCCUGC**CUGUGACuugcagugccuucacauagucauccuugc

DS B_GSTP1-1

5′-GGGAAUCC**GCAGGCU**GGAUUCCCGUCACAG**AGAACGC**CUGUGACuugcagugccuucacauagucauccuugc

DS C_GSTP1-1

5′-GGGAAUCC**GCGUUCU**GGAUUCCCGUCACAG**ACGUCUC**CUGUGACuugcagugccuucacauagucauccuugc

DS D_GSTP1-1
5′-GGGAAUCC**GAGACGU**GGAUUCCCGUCACAG**UCGUGGU**CUGUGACuugcagugccuucacauagucauccuugc
DS E_GSTP1-1
5′-GGGAAUCC**ACCACGA**GGAUUCCCGUCACAG**AACCAUC**CUGUGACuugcagugccuucacauagucauccuugc
DS F_GSTP1-1
5′-GGGAAUCC**GAUGGUU**GGAUUCCCGUCACAG**AGUGGAC**CUGUGACuugcagugccuucacauagucauccuugc
DS sense
5′-pAAGGAUGACUAUGUGAAGGCACUGC

Sense strand (underlined) concatenated with J18 aptamer selected to bind Epidermal Growth Factor Receptor (EGFR)[6]

Starting sequence (in lower case) required for high yield transcription with T7 RNA polymerase was removed post-transcriptionally using RNase H. Underlined sequence corresponds to the sense strand of DS RNA of GFP and is used for binding to RNA nanorings 3′-side functionalized with DS antisenses against GFP.

J18_sense
5′gggaaaggaagagcGGCGCUCCGACCUUAGUCUCUGCAAGAUAAACCGUGCUAUUGACCACCCUCAACACACUUAUU
UAAUGUAUUGAACGGACCUACGAACCGUGUAGCACAGCAGAUUUGACCCUGAAGUUCAUCUGCACCACCG
DNA used for RNase H mediated degradation of J18_sense starting sequence
5`-gctcttcctttccc

Fluorescently labeled sequences

All fluorescently labeled RNA and DNA sequences were purchased from IDT.

Sense strand of DS RNA duplex designed against eGFP[2]

RNA sense Alexa 546 (for in vitro uptake studies)
5`-/5AlexF546N/ACCCUGAAGUUCAUCUGCACCACCG
RNA sense IRDye700 (for in vivo studies)
5`-/5IRD700/ACCCUGAAGUUCAUCUGCACCACCG

DNA sequences designed for auto-recognizing R/DNA hybrid experiments

DNA for sense Alexa488
5′-GGAGACCGTGACCGGTGGTGCAGATGAACTTCAGGGTCAtt/3AlexF488N/
DNA for antisense Alexa546
5′-/5AlexF546N/aaTGACCCTGAAGTTCATCTGCACCACCGGTCACGGTCTCC

DNAs designed for visualization

DNA-sense-Alexa546 (for *in vitro* transfection experiments)
5′-/5AlexF546N/aaTGACCCTGAAGTTCATCTGCACCACCG
DNA-sense-IRDye700 (for *in vivo* experiments)
5`-/5IRD700/ACCCTGAAGTTCATCTGCACCACCG

Biotinilated DNAs

DNA-sense-Biotin
5′ /5Biosg/aaTGACCCTGAAGTTCATCTGCACCACCG

DNA sequences designed for auto-recognizing RNA-DNA hybrids against eGFP[7]

Auto-recognizing toe-holds are underlined.
DNA for sense (12 nts toehold)
5′-GGAGACCGTGACCGGTGGTGCAGATGAACTTCAGGGTCA
DNA for antisense (12 nts toehold)
5′-TGACCCTGAAGTTCATCTGCACCACCGGTCACGGTCTCC

SUPPORTING FIGURES

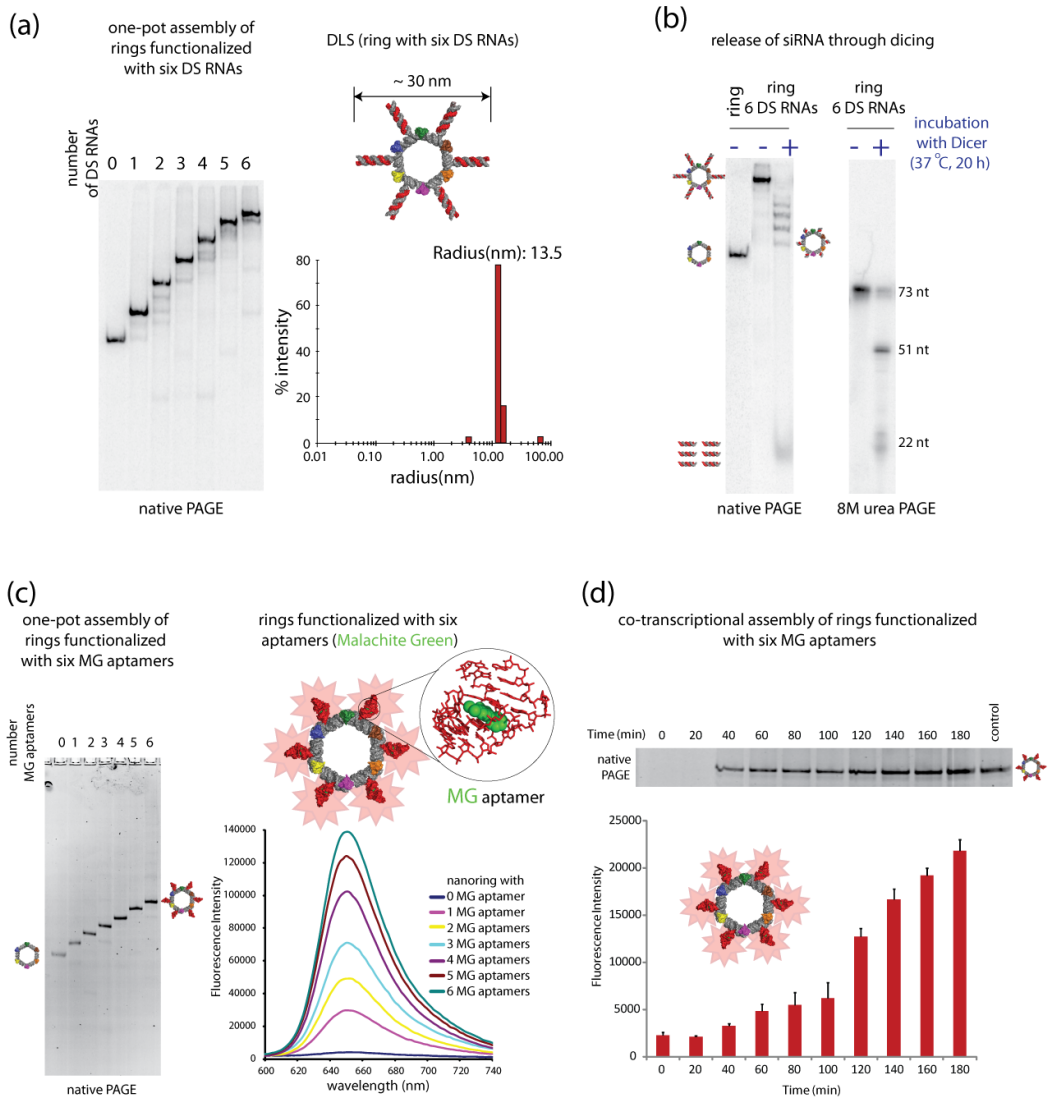

Figure S1. (**a**) Native-PAGE results representing assemblies leading to the formation of RNA nanorings functionalized with different numbers of DS RNAs (0-6). Dynamic light scattering (DLS) confirms assembly result and denotes nanoring radius. (**b**) *In vitro* dicing experiments[1]. RNA nanorings functionalized with six siRNAs were incubated with human recombinant Dicer enzyme (Methods). Constructs treated with Dicer were analyzed using native-PAGE (left) and denaturing 8M urea PAGE (right) and show successful siRNA cleavage. Non-functionalized RNA nanoring was used as a control. One-pot (**c**) and co-transcriptional (**d**) assemblies of nanorings functionalized with up to six Malachite Green (MG) aptamers. Assemblies of RNA nanorings functionalized with different numbers (0-6) of a Malachite Green (MG)-specific aptamer (PDB: 1F1T[8]) demonstrate the sequential increase in the fluorescence of MG dye. (**d**) Co-transcriptional assemblies of RNA nanorings[9] (verified by native-PAGE, on top) functionalized with six MG aptamers visualized through the increase in the fluorescence of MG dye over the transcription time (bottom graph).

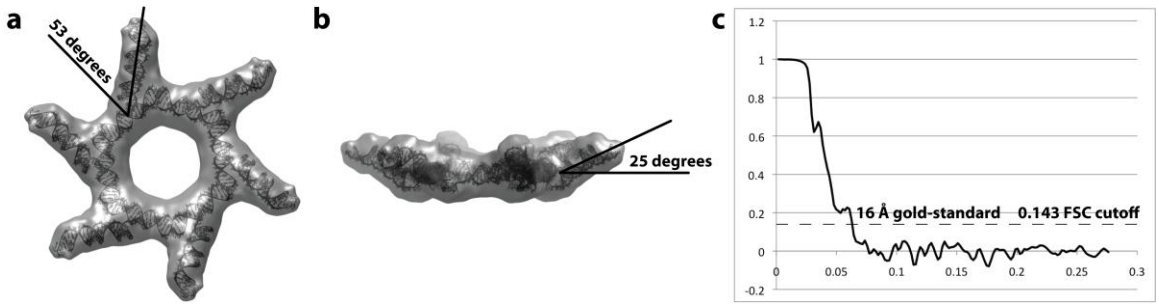

Figure S2. Cryo-EM reconstruction demonstrates that the arms in the siRNA ring do not point straight out. (**a**) Looking from the top, the DS RNA arms are positioned in a pinwheel fashion around the ring. The six DS RNA arms point about 53 degrees clockwise compared to the arms in the Figure 1 model. (**b**) Looking from the side, siRNA arms point about 25 degrees upward thus creating a crown shape of the hexagonal molecule. (**c**) The resolution of the Cryo-EM density map was assessed to be 16 Å using the gold-standard criterion of Fourier Shell Correlation (FSC) cutoff at 0.143 from two independent half-sets of data.

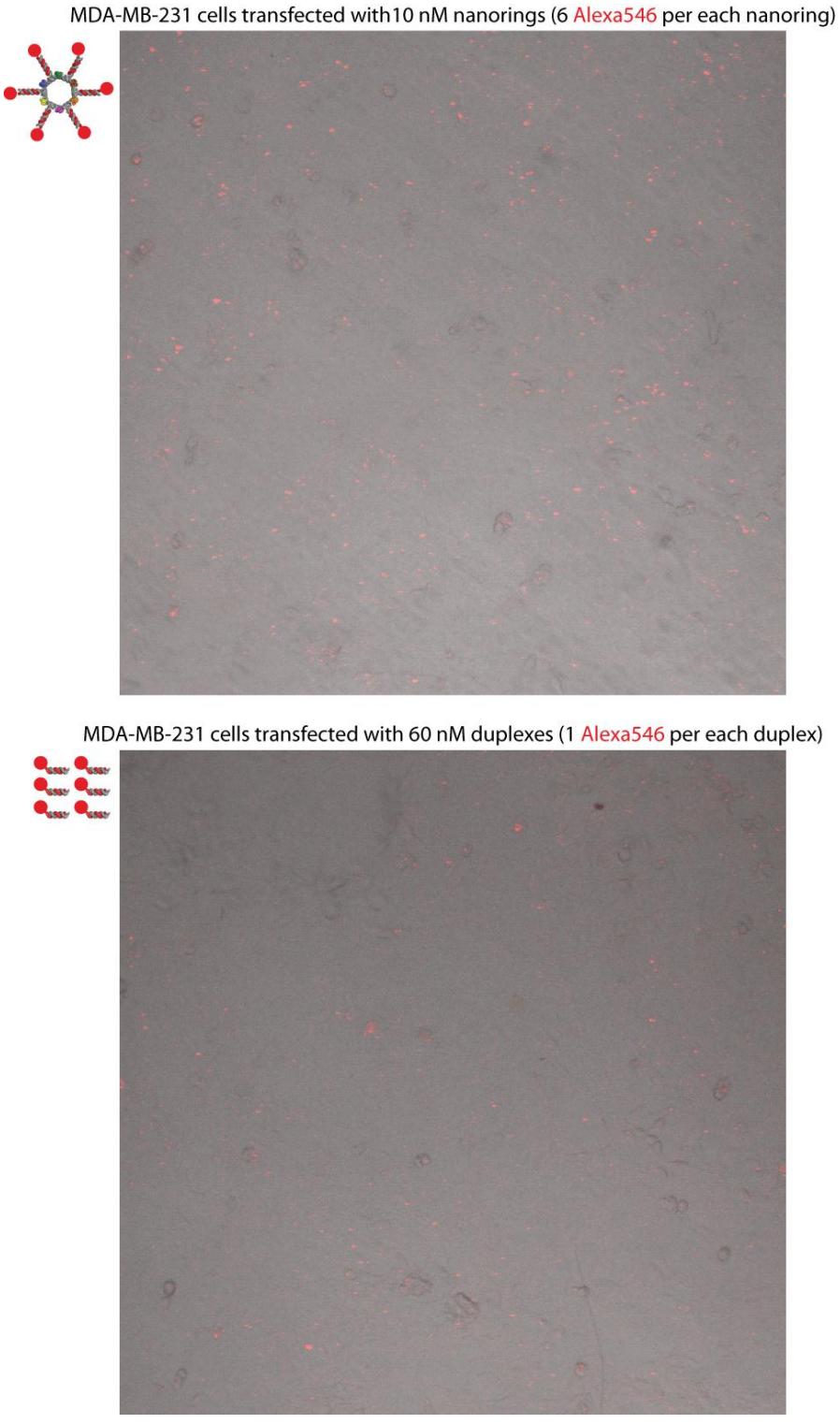

Figure S3. Relative transfection efficiencies for DS RNAs and nanorings functionalized with six DS RNAs (three independently taken images for each case). On the next day after the transfection of cells (~90% confluence) with DS RNAs and nanorings functionalized with six DS RNAs labeled with Alexa546, the efficiencies were analyzed by confocal fluorescence microscopy.

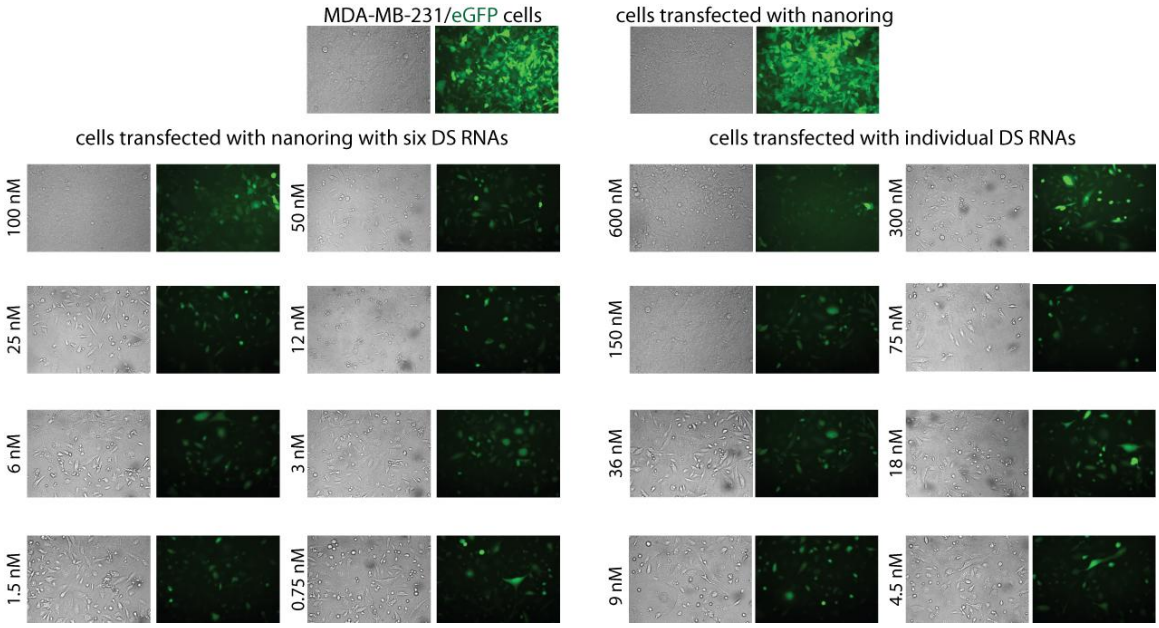

Figure S4. GFP knockdown visualization assays for human breast cancer cells (MDA-MB-231) which stably express enhanced GFP (eGFP) transfected with different concentrations of nanorings functionalized with six DS RNAs (at 100, 50, 25, 12, 6, 3, 1.5, and 0.75 nM final) and DS RNA duplexes (at 600, 300, 150, 75, 30, 15, 9, and 4.5 nM final). Note that due to the use of one-type of siRNA against eGFP, siRNA duplexes were transfected at six-fold higher concentrations compared to the corresponding functionalized nanorings. The relative levels of eGFP expression were visually analyzed for silencing of GFP expression with fluorescent microscopy three days post transfection. Note that the total number of cells per randomly selected field may vary from sample to sample.

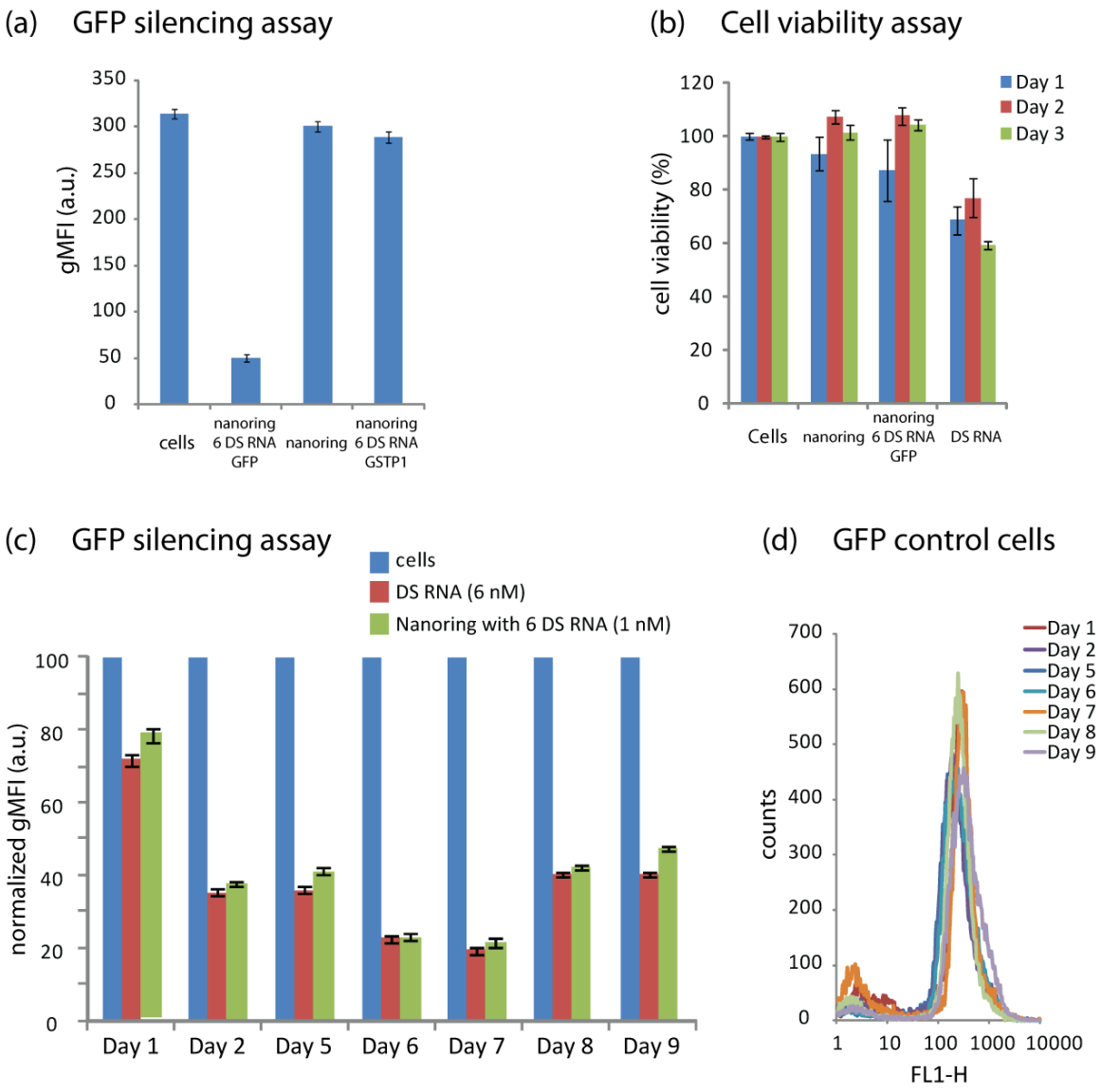

Figure S5. (**a**) GFP knockdown assays for human breast cancer cells (MDA-MB-231/GFP) which stably express enhanced GFP (eGFP) transfected with nanorings, nanorings functionalized with six DS RNAs against GFP and nanorings functionalized with six DS RNAs against GSTP1 at 100 nM each. (**b**) Cell viability assay conducted at different time points. Error bars denote SD, N=3. (**c**) GFP knockdown assays recorded at different time points for DS RNAs (at 6 nM) and nanorings functionalized with six DS RNAs (at 1 nM). The relative levels of eGFP expression were statistically (30,000 cells) analyzed with flow cytometry experiments 1 day, 2 days, 5 days, 6 days, 7 days, 8 days and 9 days post transfection. (**d**) FACS data for corresponding non-normalized control cells at different time points. In (**a**) and (**c**), gMFI corresponds to the geometric mean fluorescence intensity. Error bars denote SEM.

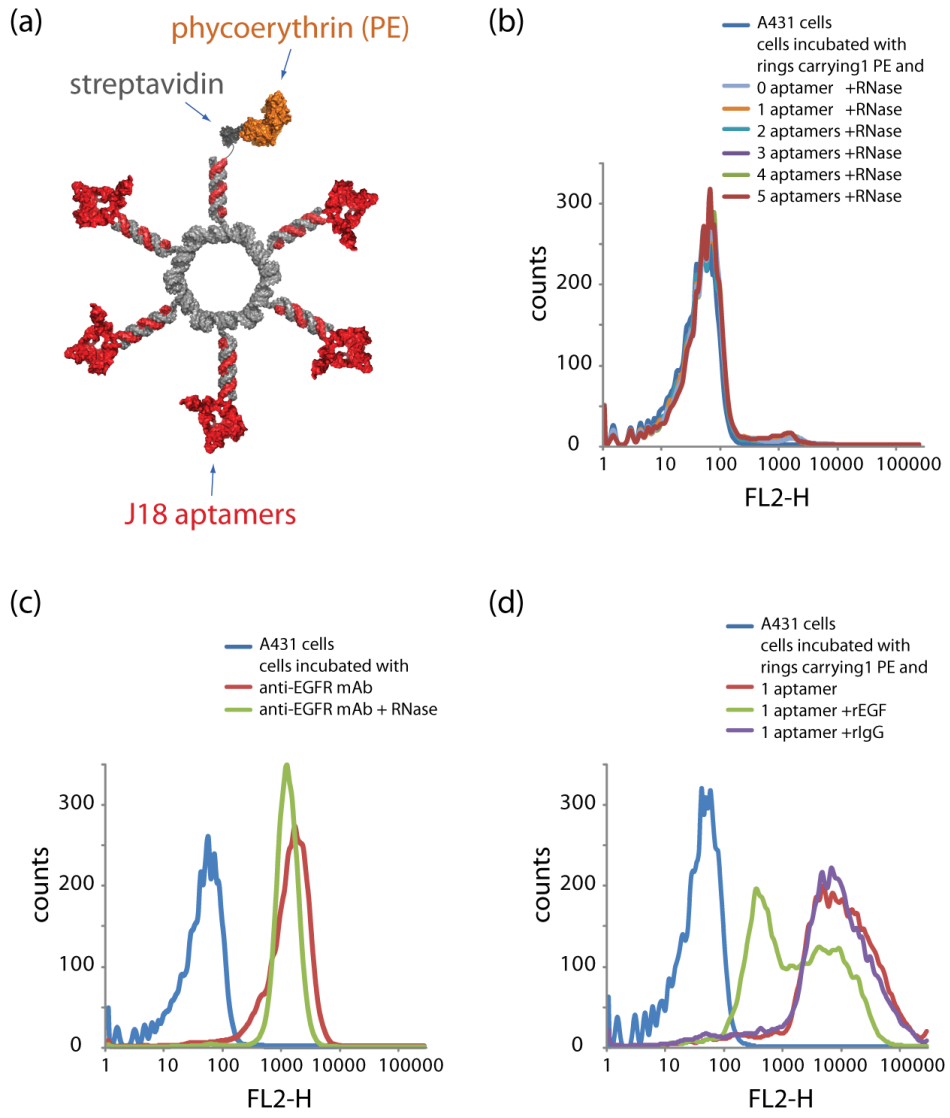

Figure S6. Nanorings functionalized with J18 aptamers bind specifically to target EGFR on A431 cells. **(a)** 3D model representing nanorings labeled with phycoerythrin (PE) and containing five J18 aptamers selected to specifically bind EGFR expressed on A431 cells. The J18 RNA aptamer model is a conceptual cartoon, based on the minimum free energy secondary structure (MFE) predicted for the sequence by the RNAfold program[10, 11] and the most compact 3D structure predicted by the RNAComposer program for this MFE[12, 13]. (**b**) Binding of NPs is mediated by RNA aptamers since the treatment with RNases resulted in a loss of the fluorescence signal. Note that the corresponding samples without RNase treatment are presented in Figure 3d. (**c**) The binding of monoclonal antibodies against EGFR. Simultaneous treatment using mAb against EGFR and RNases does not lead to loss of detection of EGFR, which confirms that loss of signal upon treatment with RNases is due to the degradation of RNA aptamers and not their target. (**d**) Competition of NP binding using rEGF resulted in a decrease of the signal as shown for a NP with one J18 aptamer. Also, the decrease of fluorescence was not caused by nonspecific degradation of RNA by the recombinant protein, because treatment with rIgG did not change the signal.

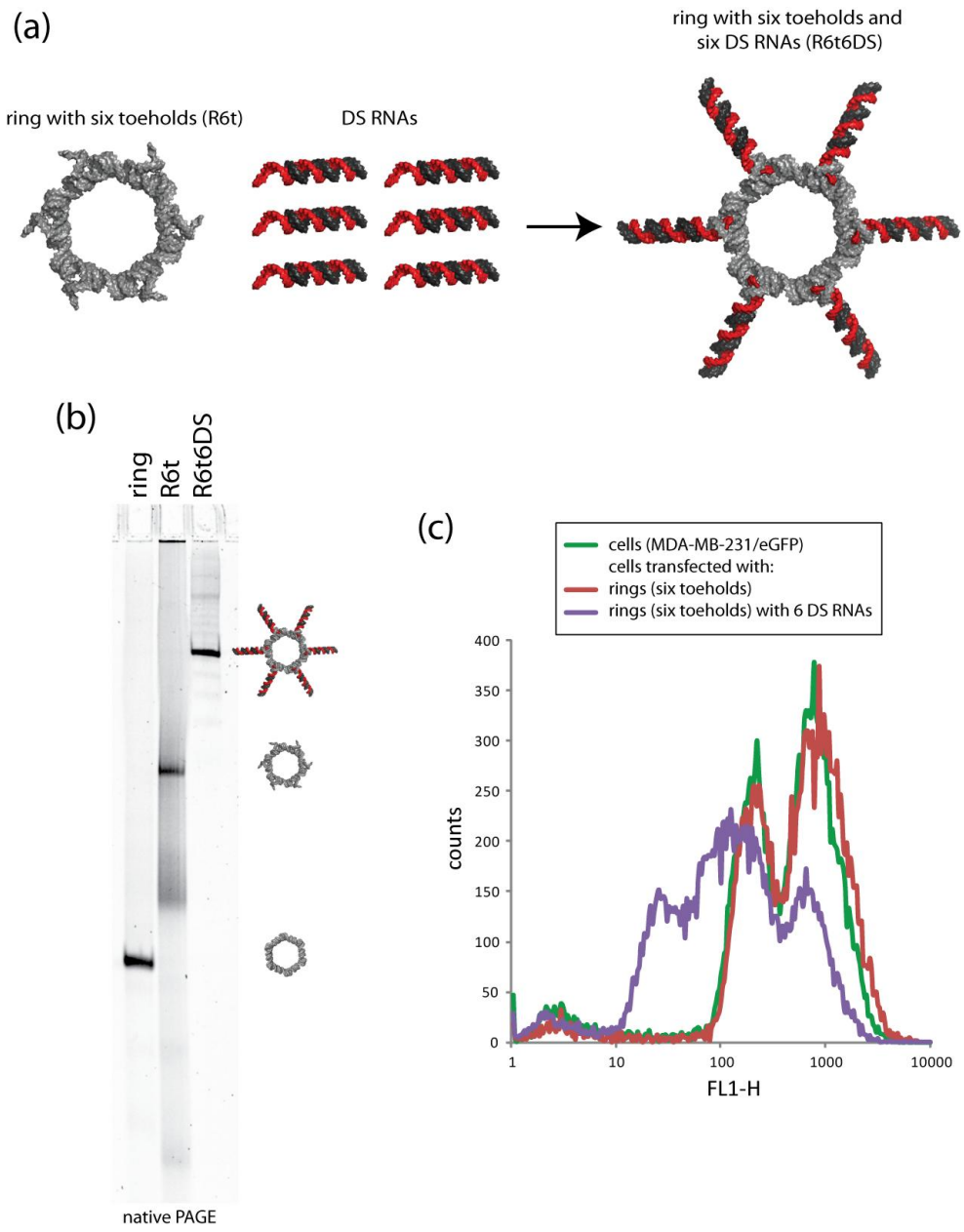

Figure S7. Functionalization of nanorings through toehold interactions. **(a)** Schematic representation of assemblies leading to the formation of RNA nanorings functionalized with six DS RNAs via toehold interactions. (**b**) Native-PAGE results representing assemblies leading to the formations of RNA nanorings functionalized with six ssRNA toeholds and six DS RNAs. (**c**) GFP knockdown assays in human breast cancer cells (MDA-MB-231/GFP) which stably express enhanced GFP (eGFP). Statistical analysis (30,000 cells per sample) of flow cytometry experiments of eGFP expression three days after the transfection of cells with nanorings carrying six toeholds and nanorings functionalized via toehold interactions with six DS RNAs against eGFP.

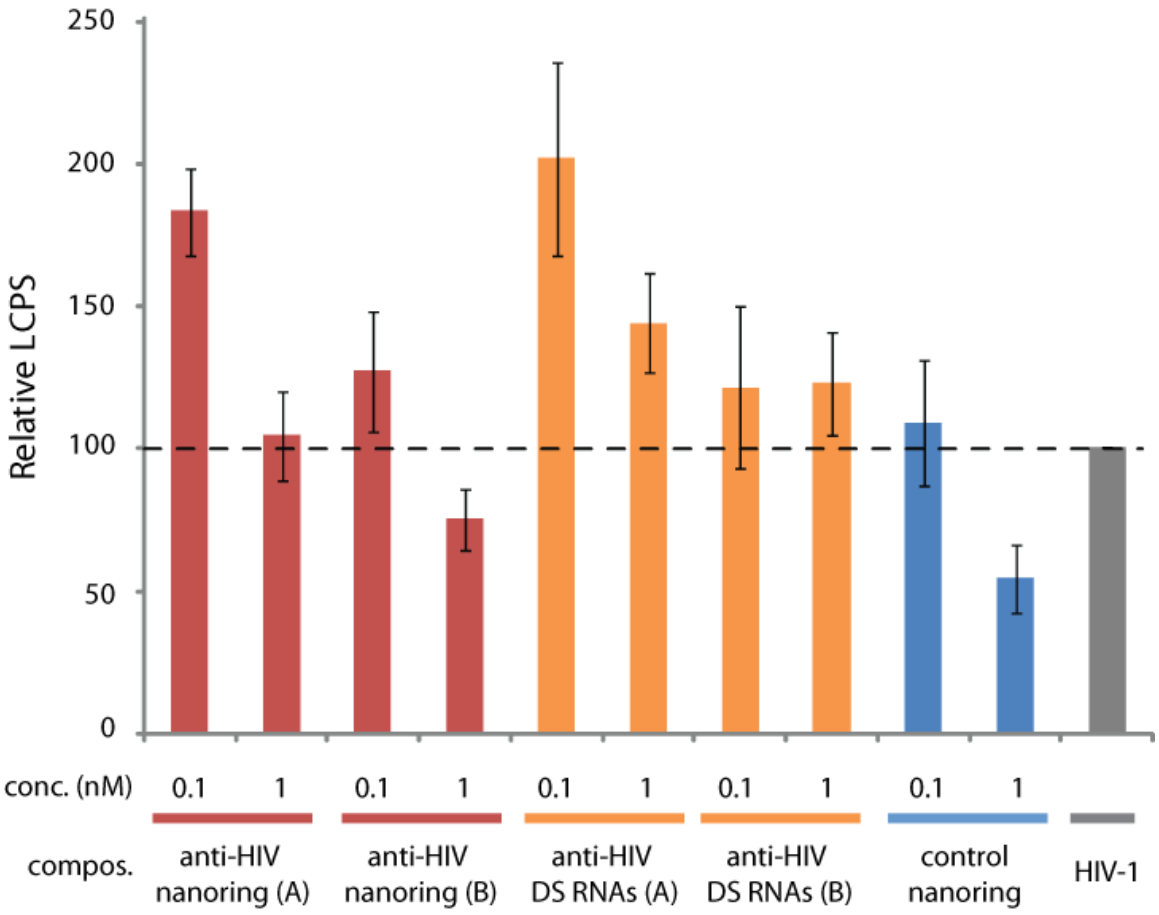

Figure S8. Cytotoxicity of functional anti-HIV nanoring constructs A and B and controls (LCPS = luciferase counts per second) in HIV-1-expressing HeLa cells. Cytotoxicity is minimal at 1nM of nanoring (B). Cells are co-transfected with pNL4-3 (HIV-1 molecular clone) and psiCHECK™-1 (Renilla Luciferase vector, Promega), with and without nanorings or dicer substrates (DS) RNAs. At 48 h post-transfection, cells were lysed and Renilla luciferase was measured. Data are shown normalized to virus controls (HIV-1). Anti-HIV DS RNAs (A and B), mixture of 6 different DS RNAs were used as positive control. Nanoring control has 6 copies of GSTP1 DS RNAs, and it was used as a negative control. HIV-1, Virus control. Error bars denote +/-SEM; N=4.

Supporting References

1. Afonin, K. A.; Grabow, W. W.; Walker, F. M.; Bindewald, E.; Dobrovolskaia, M. A.; Shapiro, B. A.; Jaeger, L., Design and self-assembly of siRNA-functionalized RNA nanoparticles for use in automated nanomedicine. *Nat Protoc* **2011,** *6*, 2022-34.
2. Rose, S. D.; Kim, D. H.; Amarzguioui, M.; Heidel, J. D.; Collingwood, M. A.; Davis, M. E.; Rossi, J. J.; Behlke, M. A., Functional polarity is introduced by Dicer processing of short substrate RNAs. *Nucleic Acids Res* **2005,** *33*, 4140-56.
3. Afonin, K. A.; Danilov, E. O.; Novikova, I. V.; Leontis, N. B., TokenRNA: a new type of sequence-specific, label-free fluorescent biosensor for folded RNA molecules. *Chembiochem* **2008,** *9*, 1902-5.
4. Grate, D.; Wilson, C., Laser-mediated, site-specific inactivation of RNA transcripts. *Proc Natl Acad Sci U S A* **1999,** *96*, 6131-6.
5. Low, J. T.; Knoepfel, S. A.; Watts, J. M.; ter Brake, O.; Berkhout, B.; Weeks, K. M., SHAPE-directed discovery of potent shRNA inhibitors of HIV-1. *Mol Ther* **2012,** *20*, 820-8.
6. Li, N.; Ebright, J. N.; Stovall, G. M.; Chen, X.; Nguyen, H. H.; Singh, A.; Syrett, A.; Ellington, A. D., Technical and biological issues relevant to cell typing with aptamers. *J Proteome Res* **2009,** *8*, 2438-48.
7. Afonin, K. A.; Viard, M.; Martins, A. N.; Lockett, S. J.; Maciag, A. E.; Freed, E. O.; Heldman, E.; Jaeger, L.; Blumenthal, R.; Shapiro, B. A., Activation of different split functionalities on re-association of RNA-DNA hybrids. *Nat Nanotechnol 8*, 296-304.
8. Baugh, C.; Grate, D.; Wilson, C., 2.8 A crystal structure of the malachite green aptamer. *J Mol Biol* **2000,** *301*, 117-28.
9. Afonin, K. A.; Kireeva, M.; Grabow, W. W.; Kashlev, M.; Jaeger, L.; Shapiro, B. A., Co-transcriptional Assembly of Chemically Modified RNA Nanoparticles Functionalized with siRNAs. *Nano Lett* **2012,** *12*, 5192-5.
10. Gruber, A. R.; Lorenz, R.; Bernhart, S. H.; Neubock, R.; Hofacker, I. L., The Vienna RNA websuite. *Nucleic Acids Res* **2008,** *36*, W70-4.
11. Lorenz, R.; Bernhart, S. H.; Honer Zu Siederdissen, C.; Tafer, H.; Flamm, C.; Stadler, P. F.; Hofacker, I. L., ViennaRNA Package 2.0. *Algorithms Mol Biol* **2011,** *6*, 26.
12. Popenda, M.; Szachniuk, M.; Antczak, M.; Purzycka, K. J.; Lukasiak, P.; Bartol, N.; Blazewicz, J.; Adamiak, R. W., Automated 3D structure composition for large RNAs. *Nucleic Acids Res* **2012,** *40*, e112.
13. Popenda, M.; Szachniuk, M.; Blazewicz, M.; Wasik, S.; Burke, E. K.; Blazewicz, J.; Adamiak, R. W., RNA FRABASE 2.0: an advanced web-accessible database with the capacity to search the three-dimensional fragments within RNA structures. *BMC Bioinformatics* **2010,** *11*, 231-242.